Title

Characterization of Fugitive Emissions From Carbon Dioxide Laser Cutting Activities

Author

Munoz, Alejandro

Publication Date

2022

Peer reviewed|Thesis/dissertation

UNIVERSITY OF CALIFORNIA

Los Angeles

Characterization of Fugitive Emissions From Carbon Dioxide Laser Cutting Activities

A thesis submitted in partial satisfaction of

the requirements for the degree Master of Science

in Environmental Health Sciences

by

Alejandro Muñoz

2022

ABSTRACT OF THE THESIS

Characterization of Fugitive Emissions

From Carbon Dioxide Laser Cutting Activities

by

Alejandro Muñoz

Master of Science in Environmental Health Sciences

University of California, Los Angeles, 2022

Professor Su-Jung Tsai, Chair

Compact laser cutters are growing in popularity and are used in a wide range of applications in many industries. Laser cutters can cut various types of materials, including metals, wood, plastics, and many others. Although many are equipped with fume extractors for removing airborne substance generated during laser cutting, there is a potential for gases and particulate matter to be released upon opening the lid after a cut has been completed. This presents the potential for laser-generated air contaminants (LGACs), in the form of particulate matter and chemical gases, into the workspace. Particulate matter refers to the solid and liquid particles suspended in the air which can be hazardous based on their size and composition. Real-time instruments were utilized to monitor both particulate concentration and size distributions, while the novel Tsai Diffusion Sampler (TDS) was used to collect particulate samples on a polycarbonate membrane and TEM

grid. Preliminary detection of released gases consisted of the use of gas sampling with Teflon Gas Bags and followed with analysis using Gas Chromatography-Mass Spectrometry (GC-MS). In addition, a portable ambient infrared air analyzer was used to quantify the concentrations of the chemicals released by the laser cutting activities. Results of the study found that a significant concentration of particulate matter ranging 15.4 - 86 nm in particle sizes can be released each time the laser cutter lid is opened and were observed to gradually increase in concentration for a period at least 20 minutes after the completion of a cut. Because of the potential and unknown toxicity of nanoparticles emitted from laser cutting, it is important to understand the trends of nanoparticles released through laser cutting activities. The GC-MS gaseous samples primarily contained methyl methacrylate at a low level close to the detection limit of the infrared air analyzer.

The thesis of Alejandro Muñoz is approved.

Yifang Zhu

Irwin H. Suffet

Su-Jung Tsai, Committee Chair

University of California, Los Angeles

2022

TABLE OF CONTENTS

LIST OF TABLES AND FIGURES

ACKNOWLEDGMENTS

Authors acknowledge the financial support to Alejandro Munoz provided by the Centers for Disease Control and Prevention through grant number 5T42OH008412-16 to Southern California Education Research Center, and the research support provided by the Department of Health and Human Services, National Institutes of Health, National Institute of Environmental Health Sciences through grant number 1R25ES033043-01 to Southern California Superfund Research Program at University of California Los Angeles. The authors also acknowledge the technical support by Judy Su at California NanoSystems Institute (CNSI) at University of California Los Angeles providing professional analysis of the particulate samples that were collected during the experimentation.

INTRODUCTION

One of the fabrication processes that is growing in popularity is the use of carbon dioxide (CO_2) laser cutters.[1] Laser cutters are used in various industries because of their ability to cut and engrave different materials at a high degree of accuracy and precision without having to constantly change tools due to wear from repetitive use.[2, 3] Because of their compact size, low cost, and reliability, these laser cutters can be placed in small classrooms, offices, and other convenient locations. Compact laser cutters produce high-intensity infrared light beams that can reach hundreds of watts/cm^2 of power density to achieve cutting and engraving material such as glass, metals, polymers, and wood. [1, 2, 3, 4] The high-intensity beams cause melting, evaporation, and volatilization of the material, which in turn generate emissions in the form of gases, chemical vapors, and particulate matter which are referred to as Laser Generated Air Contaminants (LGACs). [1, 2, 4, 5] The types of LGACs released from laser cutting will depend on various factors such as the type of material used, the speed and power at which the laser cutter is operated, and the duration of the cut. [5, 6, 7]

Local exhaust filtration systems, such as fume extractors, are available to use with laser cutters which are designed to reduce the LGACs that are emitted from cutting different materials.[8] The fume extractors are generally equipped with a series of filters and adsorbent materials, such as activated carbon, which are effective in reducing chemical and particulate emissions. [8] However, since some of the systems are connected through the back portion of the laser cutters, there is still a potential for fugitive emissions to leak out through the front when the lid is opened after a cut has been completed. The fugitive particle and chemical emissions that escape through the laser

cutter lid once the local exhaust ventilation systems have been turned off have yet to be quantified and characterized for laser cutting several types of materials, including polymethyl methacrylate.

Among the most used type of plastic material within carbon dioxide laser cutters is polymethyl methacrylate (PMMA), otherwise known as acrylic.[9] PMMA is a thermoplastic polymer that is popular due to its low cost as well as chemical and physical properties which result in high-quality cuts.[9, 10, 11, 12] It is used in dentistry, the production of electronics, greenhouses, and various other products. [9] PMMA has a rigid structure that responds well to the energy produced by CO_2 laser beams, and as a result, it can absorb laser energy quickly resulting in a faster, more precise cut. [9, 10, 11, 12] When exposed to the high heat of the laser, PMMA undergoes thermal degradation and can release methyl methacrylate (MMA), ethyl acrylate, phenols, and PAHs in addition to particulate matter. [1, 6, 13] PAHs are a group of organic compounds that can be found in the air as a result of the incomplete combustion of organic materials, with certain types identified as being carcinogenic, mutagenic, and teratogenic to humans. [14, 15, 16, 17] Particulate matter refers to the solid and liquid particles suspended in the air which can be hazardous based on their size and composition.[18] Particulates with a physical diameter of less than 100 nanometers (nm) are referred to as nanoparticles (NPs) and can be toxic in high concentrations due to the larger surface area to volume ratio compared to larger particles of the same mass. [5, 19, 20] NPs that enter the body through the inhalation pathway can deposit deep into the lungs and can cause inflammation and oxidative stress in the lungs, and lead to respiratory diseases, and other health problems. [14, 19, 20, 21] The toxicity of the NPs has been shown to vary based on the size, shape, and chemical composition, with smaller particles having a higher degree of toxicity. [15, 19]

A study by Haferkamp et al., found that laser cutting PMMA generated a higher distribution of smaller sized particles when compared to the other types of plastics, as well as high levels of PAHs.[5] The peak diameter for the PMMA generated aerosols occurred at about 0.05 μm (50 nm).[5] However, the rate of particular emissions was found to be relatively low when compared to other types of plastics. [5] The study does not make a reference to the total concentration of particulates and chemical emissions at various parts of the laser cutting process, which would be important to note in order to develop a more efficient control measure. Another study by Kiefer and Moss found that laser cutting PMMA generated particles within a 25 W CO_2 laser cutter enclosure that was more than 10 times the measured background levels.[22] This study focused on the LGACs produced within the enclosure of the laser cutter, but does not refer to the total concentration that escapes from the lid during the various phases of the laser cutting process. In addition, both studies focused on relatively short cutting times. Since emissions are dependent on an abundance of factors such as process performed, laser intensity, laser power, laser speed, and duration of the task, particulate emissions generated at different operating processes will be of concern, especially if longer cuts generate a higher concentration of LGACs.[6] This study is the first to investigate the total and size fractioned concentrations of particles and chemicals emitted from laser cutting at various phases of the laser cutting process for longer cut times, as well as using the novel Tsai Diffusion Sampler (TDS) to specifically sample and characterize nanoparticles emitted from the laser cutting.

METHODS

Study Design

This project was conducted to investigate the fugitive particulate and gas emissions released from cutting PMMA sheets with the use of a 60-W compact laser cutter. The first part of the study focused on the particulate matter emitted during and after the laser cutting process. Particulate size and range distributions were monitored with the use of real-time monitoring instruments throughout the laser cutting operation. Samples of particulate matter were collected using the Tsai Diffusion Sampler (TDS) and analyzed with microscopy. [23] The second part of the study focused on the chemical gas emissions released during the lid opening upon the completion of the cutting. Gas samples were collected using 1-L Teflon gas bags and were analyzed using Gas Chromatography-Mass Spectrometry (GC-MS) for chemical identifications. After the chemical identification, a portable infrared (IR) analyzer, which uses an infrared spectrophotometer, was used to measure the concentration in real-time. The portable analyzer includes a library of gases, and can be preset to detect certain chemicals at different wavelengths. The conditions for each experiment were kept as similar as possible, changing only the time waited before turning off the fume extractor and opening the lid of the laser after each cut. The times were chosen based on observations of the operation of the laser cutter by the users.

Facility and Equipment

The workplace which hosts the laser cutter that was observed in this study has two available CO_2 laser cutters which are spaced about 6 feet apart from each other. A desk is situated in between both laser cutters, which is where individuals that use the laser cutters can create designs and monitor their projects. In addition to the studied laser cutter, there are about 21 3D printers available to use by visitors to the facility, as well as a second laser cutter is approximately 4 feet

away from the primary laser cutter used during the experimentation. The 3D printers located in the facility primarily use the materials acrylonitrile butadiene styrene (ABS) and polylactic acid (PLA), and are located at a distance of approximately 40 feet from the laser cutter area. The area of the space is approximately 5,250 square feet and has an average ceiling height of 8 feet. The facility is equipped with two air handling units, which combine for a total of 6.5 air exchanges per hour when they are used simultaneously. The entrance to the facility is located near an industrialized area which includes a warehouse and machine shop. The air duct used for the main ventilation system is located near the front entrance of the facility, facing the industrialized alleyway. This leads to the potential concern of outside pollutants, such as diesel particulates, being ventilated indoors through both the ventilation system and the doors each time they are opened.

Laser Cutter and Materials

A 60-watt laser cutter (Universal Laser Systems, Versa LASER – VLS6.60), which produces a 10.6-micron infrared laser, was used to cut a set design into PMMA sheets measured to be 0.125 inches thick. The intensity of the laser was set at the maximum power to ensure a complete cut of the sheets. The manufacturer user interface software was used to ensure that both the design and the cutting time were kept constant. A BOFA Fume Extractor (AD 1000 IQ) is connected to the rear portion of the laser cutter as a local exhaust ventilation system to reduce the pollutants emitted from the process. The fume extractor is designed with a borosilicate pre filter that captures large particulates (95%, 0.9 μm), a combined filter that captures smaller particulates with a HEPA Filter (99.997%, 0.3 μm), and an activated carbon filter to filter out chemical gas emissions. As per

facility requirements, the fume extractor was turned on prior to starting any cut and was kept on for varying amounts of time after the completion of a cut.

Experimental Process

Particulate Monitoring Equipment and Data Analysis

The total concentration and size range distribution of particulate emissions were monitored throughout the entire laser cutting process. The instruments were set up on a cart directly in front of the laser cutter as shown in Figures S1A and S1B included in the Supporting Information (SI). A Nanoscan scanning mobility particle sizer (Nanoscan SMPS, TSI Model 3910, Shoreview, MN, USA, 10 – 420 nm, 13 channels, concentrations 0 to 10^6 particles/cm^3), abbreviated as SMPS in this study, was used to continuously monitor particles ranging from 10-420 nanometers (nm) at one-minute intervals. Tygon tubing was connected to the cyclone inlet of the instrument and placed 2.5 inches from the lid of the laser cutter as shown in Figure S1B. An optical particle sizer (OPS, TSI Model 3330, Shoreview, MN, USA, 0.3 – 10 μm, 16 channels) was used to continuously monitor particles ranging from 0.3-10 micrometers (μm) in one-minute intervals. Similarly, Tygon tubing was also connected to the inlet nozzle and placed 2.5 inches from the lid of the laser cutter. An additional OPS was placed on a nearby desk, which was measured to be 7 feet away from the studied laser cutter, and monitored particulate matter during the entire operation. Lastly, outside concentrations were monitored with an OPS for a duration of 2 hours during the same period in which experiments were conducted. The data that were collected from the SMPS and OPS were downloaded into the aerosol instrument manager (AIM) software and converted into a CSV file.

The graphs were created using Microsoft Excel. Data analysis included the two sample t-test, the Pearson's test for correlation, and the analysis of variance (ANOVA test). A one-way analysis of variance (ANOVA) test was used to analyze the difference in the group mean total particulate concentration of the data collected during the background, laser cutting, lid opening, and post background. The null hypothesis assumed that the mean total concentration would not differ among each portion of the laser cutting activity (H_0: $\mu_1 = \mu_2 = \mu_3 = \mu_4$). Differences were found to be significant at a p-value < 0.05. A Pearson's test for correlation was used to test the correlation between the particulate size range distributions during each period of the experimental period. A Pearson correlation coefficient of 1.00 signifies a strong positive correlation between the particle distribution and portion of the laser cutting activity. The two-sample t-test was used to test only between the background and post-background phases to determine if there was a significant change in particulate concentration that occurred throughout the experimental period. The change was significant at a p-value less than 0.05.

Monitoring Procedure and Sampling Methods

Particle emissions were sampled and collected throughout the entire laser cutting procedure. The monitoring was divided into 4 portions: background (20 minutes), cutting (10 minutes), lid opening, and post-background (20 minutes). The only factor that was changed was the amount of time that was waited before the fume extractor was turned off and the lid was opened (Method 1- 0 seconds, Method 2 - 30 seconds, Method 3 - 1 minute). The amount of time waited was based on observation of the amount of time users would wait before opening the lid of the laser cutter as listed in Table S1 in SI.

Particle Sampling and Analytical Methods

The TDS was used to collect samples of particulate matter in the respirable size range. The TDS can be used to collect the particles directly onto a polycarbonate (PC) membrane filter and transmission electron microscopy (TEM) grid.[23] The membrane filter used was a 25-mm diameter, 0.22 μm pore size polycarbonate membrane, and a TEM-copper grid in 400 mesh with the carbon-coated film was placed at the center of the filter.[23] The TDS was used with a Gilian GilAir Plus sampling pump calibrated to a flow rate of 0.9 L/min. The TDS was placed facing horizontally at 2.5 inches from the laser cutter lid. The particles collected on the TEM grid were analyzed using an FEI Tecnai T12 transmission electron microscope (Tecnai T12, FEI, Oregon) operated at an electron tension of 120 kV at various levels of magnification.

Gas Sampling and Analysis

Samples of the fugitive gas emissions were collected during the lid opening using a manual 1-liter pump along with 1-liter Teflon gas bags from Jensen Inert Products (Coral Springs, FL). The chemical gas samples were extracted from the bag using solid phase microextraction (SPME) which is based on the principle of adsorption and absorption and is widely used in the analysis of environmental pollutants in water, soil, and air. [24, 25] In the SPME method, the analytes are extracted from the gaseous media by using a coated fiber within a syringe. [24, 25] The analyte is then injected into a gas chromatograph (Varian 450, Varian Inc, California) equipped with a mass spectrometer (Varian 220, Varian Inc, California). The computer software program was used to analyze the chromatograms to determine any chemical constituents. To assess the real time

concentration of any identified chemical gases, a portable infrared ambient air analyzer (MIRAN 205B Series SapphIRe, ThermoElectron, Massachusetts) was utilized. The SapphIRe was preset to monitor the chemical MMA at two different wavelengths (10.7 and 12.3 microns) It measured the concentration in parts per million (ppm) of the selected chemical gas every 30 seconds in real time.

RESULTS AND DISCUSSION

Airborne Particles Released from Laser Cutting Activities

Changes in the total particle concentration and distribution were observed during the four stages of the laser cutting activities (background, laser cutting, lid opening, and post background). Figures 1A and 1B illustrate the changes in total particulate concentration for each experimental method as measured by the real-time instruments. The background values varied depending on the days and time that experiments were conducted since other processes in the facility, such as 3D printing, can also generate and release particulates into the ambient air. It was noted that there was an average of five 3D printers in operation during each of the experimental periods. However, based on the data that was collected, it was observed that the second laser cutter was more likely to influence spikes in particulate concentration, not the 3D printers. The use of the second laser cutter, which is approximately 4 feet from the studied laser cutter, and 6 feet from the OPS, corresponded with several spikes in concentrations, such as the ones seen during the background and laser cutting phases seen in Figure 1B.

Total Concentration and Distribution in 10-420 nm Sized Particles

Based on the graph illustrated in Figure 1A, a steady, gradual increase in total particulate concentrations was observed during the 20-minute post-background period, after the laser cutting had been completed, and the fume exhaust was turned off. An ANOVA statistical test was used to determine that there was a significant difference between the total concentration means of each phase of the laser cutting activities (Method 1: p-value=1.75×10^{-11}, Method 2: p-value= 4.4×10^{-17}; Method 3: p-value= 3.9×10^{-16}). A follow-up t-test between background and post-background total particle concentrations determined that there were only significant differences between the total background and post-background concentrations in Methods 2 and 3 (p-value = 2.3×10^{-14} and p-value = 1.8×10^{-13}, respectively). The significant increase in concentrations for particulates in the 10-420 nm size range is observed to occur after the opening of the lid, during the post-background period, showing that fugitive particulates are being released each time the lid is opened after a cut is complete. It is also observed that the highest concentration of particles was measured during the post background period across all three experimental methods (Method 1 - 18,143 particles/cm^3; Method 2 - 3,515 particles/cm^3; Method 3 - 16,190 particles/cm^3), thus further supporting the hypothesis that fugitive particulate matter was escaping after the opening of the lid.

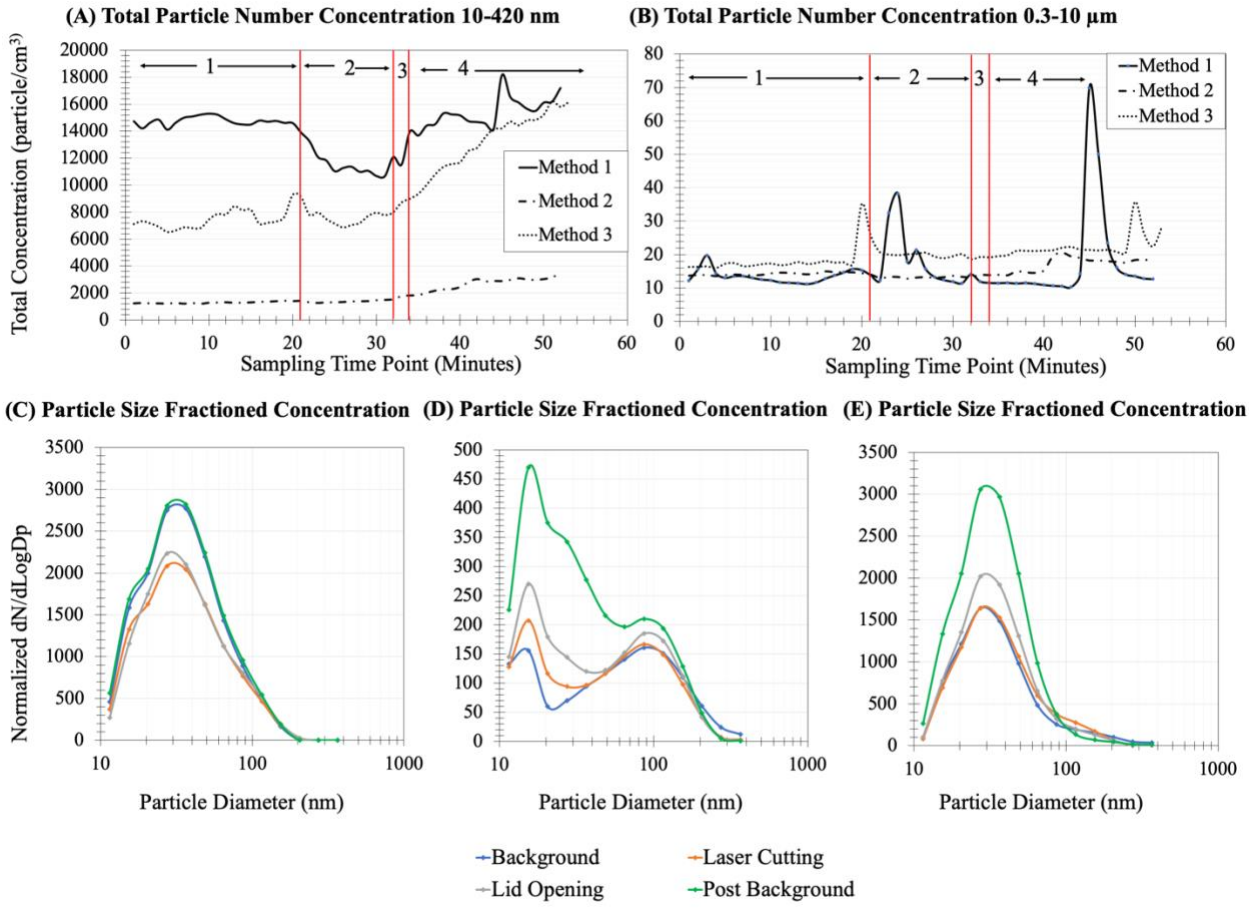

Figure 1. The total concentration of particulate matter during the four different periods of the experimentation was (1) background, (2) laser cutting, (3) lid opening, and (4) post-background. **(A)** The total concentration of particulates with diameters ranging from 10-420 nm as measured by the Nanoscan SMPS **(B)** Total concentration of particulates with diameters ranging from 0.3-10 µm as measured by the OPS. **(C-E).** Particle size fractioned concentrations (dN/dLogDp) measured by the NanoScan SMPS during each phase of the laser cutting activity (C) Size distribution for Method 1 (D) Size distribution for Method 2 (E) Size Distribution of Method 3. Note: Concentrations are normalized data.

This gradual increase during the post-background period was initially hypothesized to be attributed to the agglomeration effect within the nanoparticles. However, the particle distribution graphs (Figures 1C-E) demonstrated that the particle size distribution remained the same throughout the entire experimental period. Statistical analysis (Pearson's correlation) used to compare the particle size distributions during each of the portions of the laser cutting confirmed a high degree of correlation between each of the phases of the laser cutting activity of Methods 1, 2, and 3 in all particulate sizes measured by the NanoScan SMPS (SI Tables S2 - S9). Thus, the correlation between the distribution of particle sizes can be taken to mean that the laser lid opening did not result in the emission of particulate matter different in sizes from that which was already observed in the background measurements. If the increase had been in fact due to the agglomeration of smaller particles, then an increase in larger-sized particles would have been observed during the lid opening and post-background phases of the laser cutting activity. Despite the lack of change in size distributions, there is still a noticeable increase in particulate emissions during the post background period among all three of the experimental methods. Particles ranging from 27.4 - 36.4 nm were found to have the highest concentration during all stages of the laser cutting activities. The highest peak concentration for particles in this range were 2,821 and 3,057 particles/cm^3 for Methods 1 and 3 respectively during the post-background phase of the laser cutting activity. However, during experimental Method 2, there was a bimodal distribution observed. The distribution was highest for particles with diameters of 15.4 nm and 86 nm. The peak concentration observed during the post-background phase for particles in this size range was 470 particles/cm^3.

Total Concentration and Distribution in 0.3-10 µm Particles

The opposite trend is seen for particulate matter ranging from 0.3-10 μm as seen in Figure 1B. In contrast to the gradual increase seen for smaller particles, the concentrations within the size range would normalize almost immediately after peaking. As mentioned previously, the OPS was more susceptible to interferences from the second laser cutter that was operated at certain times during the experimental period. This type of interference is seen in Figure 1B when there are clear peaks that occur during the background and laser cutting periods of the experimental period. An ANOVA test identified that there was a significant difference in the means of the background, laser cutting, lid opening, and post-background concentrations in the experimental methods 2 and 3, but no significant difference between means in method 1 (Method 1: p-value= 0.47; Method 2: p-value= 2.42×10^{-8}; Method 3: p-value= 2.95×10^{-3}).

The distribution of particle sizes monitored by the OPS (0.3-10 μm) remained similar among all experimental methods (S.I. Figure S3). The graphs were skewed to the right, with the smallest particles (0.35 μm) having the highest distribution. The peak concentration reached in this size range was 69, 101, and 123 particles/cm^3 during methods 1, 2, and 3 respectively during the post-background period. The same statistical analysis (Pearson's correlation) was used to compare the particle size distributions during each of the portions of the laser cutting as was used for the SMPS data (S.I. Table S5-S7). The particle size distributions had a high degree of correlation during each phase of the laser cutting activity. This once again shows that the operation or opening of the laser cutter did not result in a change in particle size distributions.

Total Concentration and Distribution in 0.3-10 μm Particles from a Distance

A set of data was collected using the OPS from a desk approximately 7 feet from the laser cutter. The sample was taken concurrently with another OPS set at a distance 2.5 inches from the lid of the laser cutter (SI Figure S4). The most noticeable observation was that neither the OPS located 2.5 inches from the laser cutter, nor the one located 7 feet away, measured an increase in total particle concentrations when the lid was opened after the 1st (primary) laser cutter had completed a 10-minute cut. However, a peak in particulate data was observed at both locations during the post-background period, which was a result of the second laser cutter being used. The second laser cutter was also utilized to cut a piece of acrylic, but the process only lasted for about 2 minutes, followed by a period during which the operator left the lid open for approximately 90 seconds. The distance of both OPSs from this second laser cutter was approximately 7 feet yet the increase in concentrations was significant, reaching concentrations of 130 particles/cm^3. Because of this clear spike in concentrations from a further distance, future research should focus on setting up multiple instruments at several locations and observe the way that time of cut may influence these concentrations.

There were certain limitations that existed with the data that was collected among all experimental trials. The most important to note is that the environment in which data was collected resembled that of a field study. Since the facility could not be used outside of the normal hours of operations, the results could have been influenced by the number of times the door was opened, the number of persons within the facility, the operation of other equipment such as laser cutters and 3D printers, and other factors. In the future, it would be of greater benefit to operate the experiments in a more controlled environment. Despite these factors, based on the data that was collected by both real-time instruments, most particles that were released by the laser cutting

activities were predominantly in the nanometer-sized range. This emphasizes the need to further characterize the particles. Characterization of particle size and morphology is discussed in the next section.

Characterization of Particle Size and Morphology

The particles sampled near the laser cutting processes varied in size and shape, as seen in Figure 2. The images included were representative of particulate matter seen across all the laser cutting experiments that were conducted. The TEM images were arranged according to the experimental method during which they were captured. Figures 2A-C were included to illustrate the observed particle concentration and sizes throughout all the experimental methods. Each experimental method would result in a high concentration of smaller sized particulates (Figure 2A), while larger size particles (Figure 2B) were not as frequent, but still observed. This corresponds with the findings of the distribution graphs discussed earlier, as smaller particles were highly distributed.

According to Ott et al. (2021), in brightfield imaging, darker images indicate that electrons are not able to pass through the sample, thus indicating that the particle has a higher degree of thickness in comparison to the lighter images.[26] An example of the varying degrees of thickness captured in the samples can be observed between Figure 2E and 2I, which are two particles that appear to have a similar shapes, but Figure 2I would be considered to be much thicker based on the darkness of the particle.

The particles observed in Figures 2E-G, and 2I-K were representative of the most common type of particulate that was observed in the samples collected in each of the experiments. The particles

varied in apparent thickness and diameter with some reaching upwards to 10 µm in diameter. They closely resemble particles that are seen and described by Ott et al. as being mineral dust particles, which are made up of a combination of different mineral species. [26, 27] According to Ott et al, these types of aerosols are the second largest emissions by mass into the Earth's atmosphere. [26, 27] Therefore, it is likely that some of these particles were collected from the ambient environment.

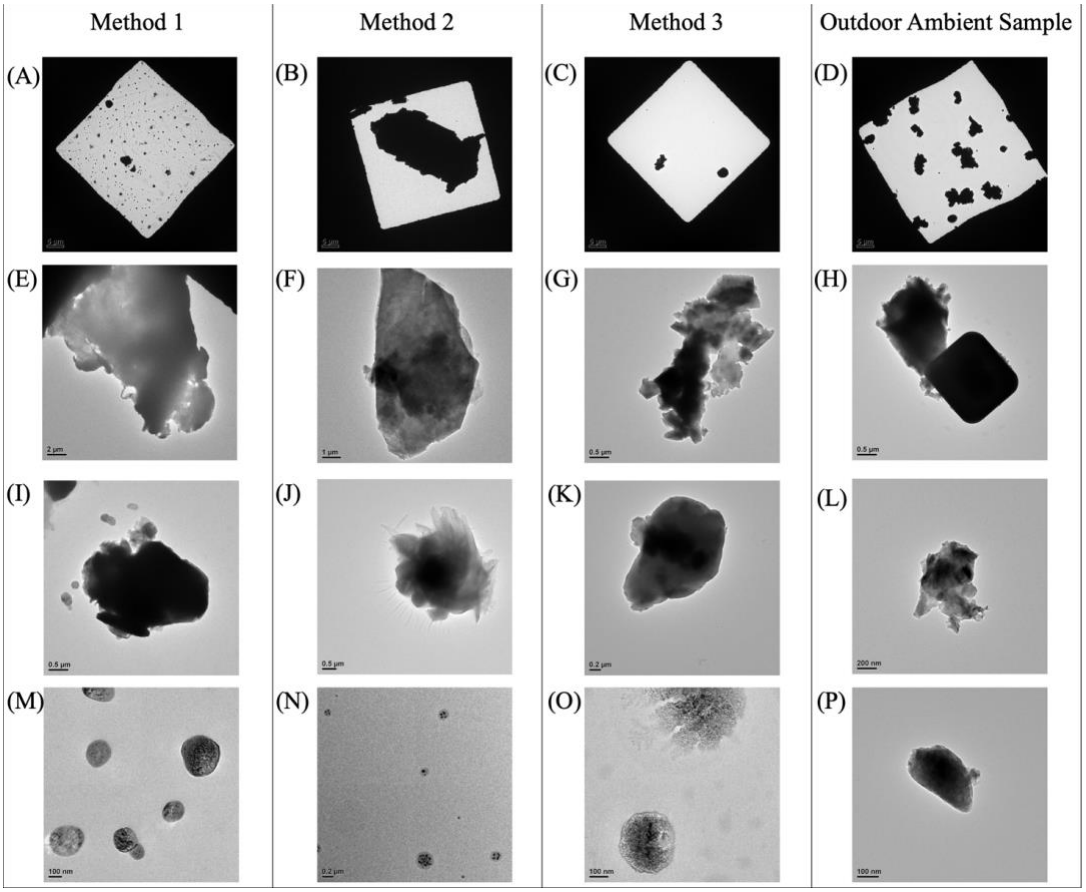

Figure 2. TEM images of the structure and size of particulates were captured using the T12 microscope contained on a carbon coated, TEM copper grid which were collected during the experimental periods and an ambient outdoor sampling period. (A-D) Represent the range in sizes collected and observed on a single TEM Grid during all of the sampling periods. (E-L) Particulates

captured among all sampling periods that closely resemble the mineral dust particles. (M-P) Particles captured during all sampling periods with TEM that resemble organic/inorganic containing particles. Note: The scale bar is 5 µm on Figures 2A-D; 2 µm on Figure 2E; 1µm on Figure 2F; 0.5 µm on Figures 6G-J; 0.2 µm on Figures 2K, 2N; 200 nm on Figure 2L and 100 nm on Figures 2M, 2O, and 2P. Images D,H, L, & P correspond to the collected outdoor ambient air samples. The rest of the images correspond to those collected from the experimental methods.

Another type of particle that appeared within the sample is seen in Figures 2M-O. The circular particles varied in size, with some having a diameter as small as 100 nm. Based on reference images, these appear to have the same characteristics as those described as organic/inorganic-containing particles in Ott et al (2021). [26, 27] However, it is important to note that the true particle size and diameter may have been altered when being observed under the TEM. The surface texture, which appears to be bubbly, may have been the result of electron beam damage undergone during the magnification of the sample. [26]

Ambient Outdoor Particulates

An additional set of data was collected with an OPS at an outside location 5 feet from the door of the facility where the laser cutter was located. The instrument measured continuously for a total of two hours from the hours of 9-11 AM, as this was the time during which the experiments were conducted (SI, Figure S4). During the two-hour period, there were several peaks in total particulate concentration that reached as high as 55 particles/cm^3 in the size range of 0.3-10 µm. Peaks in the concentration could be attributed to several factors, including the presence of vehicles that pass by

frequently to access a nearby warehouse. The particle size distribution was skewed to the right, with particles with 0.35 µm having the highest concentrations. The highest peak concentration in that size range reached 50 particles/cm^3.

The particles that were observed on the outdoor sample (Figure 2D, 2H, 2L, 2P) had many similarities to those that were captured during the laser cutting activities. The diameter size of the captured particles ranged anywhere from 100 nm to 10 µm. The samples seen in Figures 2H, L, P also closely resembled the mineral dust particles mentioned in Ott et al (2021). [26, 27] However, there were larger agglomerates that were visible, such as the one seen in Figure 2H, where the attached particle has a square shape.

Gas Sampling and Chromatography

Gas samples were collected on two separate occasions using a manual pump and a 1-L Teflon gas bag (Jensen Inert Products, Coral Springs, FL). The first sample was collected while no laser cutting activities were in progress as a reference sample. The second gas sample was collected during the lid opening portion of the laser activity. There were no identifiable chemical contaminants through analysis of the background sample. During the lid opening portion, the chemical MMA was the only chemical that was identified (CAS 80-26-6). MMA is an organic compound that is formed when PMMA undergoes thermal degradation. [28] Exposure to high concentrations of MMA can lead to irritation of the skin, eyes, and mucous membranes in humans.[28] Additionally, chronic inhalation has been documented to result in respiratory and nasal symptoms, reduced lung function, and even cardiovascular disorders in humans. [28] Since the

chemical was identified during the gas sampling, it signified that fugitive gas emissions are being released during the lid opening portion of laser activities, despite the use of a fume extractor during the process. MMA is described as having an acrid, repulsive odor, which was noticed during the laser cutting activity. [25]

Through analysis of the ambient air using the IR analyzer, it was discovered that despite the strong odor released from laser cutting PMMA, the concentrations of MMA were at or below the detectable range (0.4 ppm). The strong odor that was observed can be attributed to the relatively low odor threshold of MMA which is 0.08 parts per million (ppm). [28] To compare with the MMA concentrations outside of the facility, the IR analyzer was used to sample the outside ambient air as well (5 feet away from the entrance). The comparisons between the measured concentrations of MMA in the indoor and outdoor environment are shown in Figure 3.

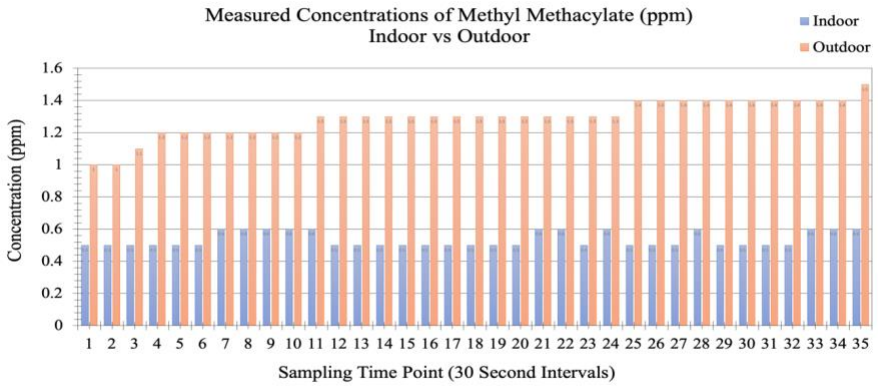

Figure 3. Concentrations of methyl methacrylate (MMA) in ppm present in indoor environments during laser cutting activities compared to the outside ambient air.

Despite MMA being identified using the preliminary GC-MS analysis, the concentrations that were measured were well below the 100 ppm Permissible Exposure Limit (PEL) set by the Occupational Safety and Health Administration (OSHA). The measured indoor concentrations (mean - 0.5 ppm), and the outside concentrations (mean - 1.3 ppm) are both considered to be well below the OSHA PEL. Based on the outside air concentrations, it is possible that the indoor levels of MMA could have also been brought in from the outside. Indoor MMA concentrations could have been a result of the frequent door opening that occurred, or from the ventilation system itself. The air duct for the ventilation system, which uses outside air, faces an industrialized area and is located at the floor level. Contaminants generated from the outside can be sucked into the facility via the ventilation system. Regardless of where the MMA was produced, it can be concluded that the fugitive gas emissions released by the laser cutter are not at a concentration high enough to cause concern under the studied operating conditions.

CONCLUSION

As a result of this study, it was determined that the fume extractor is efficient at capturing the gas emissions produced from laser-cutting PMMA material. Previous studies had reported concern about MMA emission, yet our results revealed the MMA emission was close to the detection level, showing that the fume extractor was efficient at capturing the chemical gases. [5, 22] However, the opening of the lid can result in high peak concentrations of fine and ultrafine particulate matter, which can deposit deep into the lungs and may contribute to potential health problems. Previous studies had shown that particulate emissions for laser cutting PMMA were not as high as other

types of plastics, yet there was still a significant increase found even after the usage of the fume extractor. [5, 22] The amount of fugitive particulate matter released will vary on factors such as cut time and design, and more research would be needed to determine which cut style may produce the highest concentration of particulates. One potential solution that can be applied is to keep the fume extractor on for a few minutes after the cut has been completed in order to give it time to fully filter the contaminants that are being produced by the laser cutting activity. It was noticed that during each of the experiments, during the laser cutting portion, the concentrations of particulate matter would stay at a constant level, which can be hypothesized to be contributed by the fume extractor. It is not until the fume extractor is turned off that the concentration of particulate matter, especially those in the nanometer-sized range, begins to gradually increase. The results indicate that despite the use of the fume extractor, significant concentrations of particulates with a majority in the sizes of with peak size at 27.4 - 36.4 nm above 2,821 and 3,057 particles/cm^3 (for Methods 1 and 3 respectively) in concentration are being released after the lid is opened to retrieve the finished product. Special attention should be paid to particle concentrations during the time period after the laser cutting has been completed, especially if the laser cutter is used frequently. These nanometer-sized particles appear to have a delayed release from the laser cutter, and can continuously increase in concentrations if proper ventilation systems are not in place.

AUTHOR INFORMATION

Corresponding Author

Su-Jung Tsai

Present Addresses

650 Charles E. Young Drive S., MC 177220, Los Angeles, California 90095-1735

Department of Environmental Health Sciences, Fielding School of Public Health, University of California, Los Angeles

Author Contributions

The authors note that there are no conflicts of interest. The manuscript was written through the contributions of all authors. All authors have given approval to the final version of the manuscript. Conceptualization and methodology A.M; Investigation and formal analysis, A.M Writing–original draft preparation, A.M.; Writing–review and editing, C.S.J.T., J.S., M.S, A.M.; Supervision, C.S.J.T, J.S; Project administration, C.S.J.T. All authors have read and agreed to the published version of the manuscript. The contents are solely the responsibility of the authors and do not necessarily represent the official views of the University of California, Los Angeles, or funding agencies.

Funding Sources

The Centers for Disease Control and Prevention through grant number 5T42OH008412-16 to Southern California Education Research Center, and the Department of Health and Human Services, National Institutes of Health, National Institute of Environmental Health Sciences

through grant number 1R25ES033043-01 to Southern California Superfund Research Program at University of California Los Angeles.

ACKNOWLEDGMENT

Authors acknowledge the financial support to Alejandro Munoz provided by the Centers for Disease Control and Prevention through grant number 5T42OH008412-16 to Southern California Education Research Center, and the research support provided by the Department of Health and Human Services, National Institutes of Health, National Institute of Environmental Health Sciences through grant number 1R25ES033043-01 to Southern California Superfund Research Program at University of California Los Angeles. The authors also acknowledge the technical support by Judy Su at California NanoSystems Institute (CNSI) at University of California Los Angeles providing professional analysis of the particulate samples that were collected during the experimentation.

ABBREVIATIONS

LGACs, laser generated air contaminants; TDS, Tsai Diffusion Sampler; GC-MS, Gas chromatograph – mass spectrometry; PAHs, polycyclic aromatic hydrocarbons; nm, nanometers; μm, micrometers; NPs, nanoparticles; PMMA, polymethyl methacrylate; MMA, methyl methacrylate; CO_2, carbon dioxide; HEPA Filter, high efficiency particulate air filter; SMPS, scanning mobility particle sizer; OPS, optical particle sizer; AIM, aerosol instrument manager; PC, polycarbonate; TEM, transmission electron microscopy; SPME, solid phase microextraction; PLA, polylactic acid; ABS, acrylonitrile butadiene styrene; ANOVA, analysis of variance; IR,

infrared; OSHA, Occupational Safety and Health Administration; PEL, permissible exposure limit; CNSI, California NanoSystems Institute

Supporting Information

Table S1. Correlation analysis between the background, laser cutting, lid opening, and post background of the SMPS data for experimental method 1.

Method 1- SMPS		**Background**	**Laser Cutting**	**Lid Opening**	**Post Background**
Background	*Pearson*	1.000	0.998	0.994	0.999
	P-Value	2.2 E -16	4.9 E - 14	6.8 E -12	2.2 E -16
	N	13	13	13	13
Laser Cutting	*Pearson*	0.998	1.00	0.995	0.998
	P-Value	4.9 E - 14	2.2 E -16	1.4 E -12	9.6 E -15
	N	13	13	13	13
Lid Opening	*Pearson*	0.994	0.995	1.00	0.993
	P-Value	6.8 E -12	1.4 E -12	2.2 E -16	2.0 E -11
	N	13	13	13	13
Post Background	*Pearson*	0.999	0.998	0.993	1.00
	P-Value	2.2 E -16	9.6 E -15	2.0 E -11	2.2 E -16
	N	13	13	13	13

Table S2. Correlation analysis between the background, laser cutting, lid opening, and post background of the SMPS data for experimental method 2.

Method 2 - SMPS		**Background**	**Laser Cutting**	**Lid Opening**	**Post Background**
Background	*Pearson*	1.00	0.920	0.801	0.500
	Sig.	2.2 E -16	8.5 E -6	9.9 E -4	0.08
	N	13	13	13	13
Laser Cutting	*Pearson*	0.920	1.00	0.968	0.773

	Sig.	8.5 E -6	2.2 E -16	6.4 E -8	1.9 E -3
	N	13	13	13	13
Lid Opening	*Pearson*	0.801	0.968	1.00	0.892
	Sig.	9.9 E -4	6.4 E -8	2.2 E -16	4.2 E -5
	N	13	13	13	13
Post Background	*Pearson*	0.500	0.773	0.892	1.00
	Sig.	0.08	1.9 E -3	4.2 E -5	2.2 E -16
	N	13	13	13	13

Table S3. Correlation analysis between the background, laser cutting, lid opening, and post background of the SMPS data for experimental method 3.

Method 3 - SMPS		**Background**	**Laser Cutting**	**Lid Opening**	**Post Background**
Background	*Pearson*	1.00	0.994	0.995	0.993
	Sig.	2.2 E -16	6.7 E -12	2.7 E -12	1.5 E -11
	N	13	13	13	13
Laser Cutting	*Pearson*	0.994	1.00	0.997	0.991
	Sig.	6.7 E -12	2.2 E -16	1.6 E -13	6.8 E - 11
	N	13	13	13	13
Lid Opening	*Pearson*	0.995	0.997	1.00	0.997
	Sig.	2.7 E -12	1.6 E -13	2.2 E -16	1.0 E -13
	N	13	13	13	13
Post Background	*Pearson*	0.993	0.991	0.997	1.00
	Sig.	1.5 E -11	6.8 E - 11	1.0 E -13	2.2 E -16
	N	13	13	13	13

Table S4. Correlation analysis between the background, laser cutting, lid opening, and post background of the OPS data for experimental method 1.

Method 1 - OPS		**Background**	**Laser Cutting**	**Lid Opening**	**Post Background**
Background	*Pearson*	1.00	0.995	0.998	0.994
	Sig.	2.2 E -16	2.1 E -11	9.8 E -14	6.8 E -11
	N	12	12	12	12
Laser Cutting	*Pearson*	0.995	1.00	0.993	0.999
	Sig.	2.1 E -11	2.2 E -16	1.8 E -10	2.2 E -16
	N	12	12	12	12
Lid Opening	*Pearson*	0.998	0.993	1.00	0.990
	Sig.	9.8 E -14	1.8 E -10	2.2 E -16	6.9 E -10
	N	12	12	12	12
Post Background	*Pearson*	0.994	0.999	0.990	1.00
	Sig.	6.8 E -11	2.2 E -16	6.9 E -10	2.2 E -16
	N	12	12	12	12

Table S5. Correlation analysis between the background, laser cutting, lid opening, and post background of the OPS data for experimental method 2.

Method 2 - OPS		**Background**	**Laser Cutting**	**Lid Opening**	**Post Background**
Background	*Pearson*	1.00	0.999	0.999	0.999
	Sig.	2.2 E -16	2.2 E -16	2.2 E -16	3.8 E -16
	N	12	12	12	12
Laser Cutting	*Pearson*	0.999	1.00	0.999	0.999
	Sig.	2.2 E -16	2.2 E -16	2.2 E -16	3.3 E -16
	N	12	12	12	12
Lid Opening	*Pearson*	0.999	0.999	1.00	0.999
	Sig.	2.2 E -16	2.2 E -16	2.2 E -16	3.2 E -16
	N	12	12	12	12
Post Background	*Pearson*	0.999	0.999	0.999	1.00

	Sig.	3.8 E -16	3.3 E -16	3.2 E -16	2.2 E -16
	N	12	12	12	12

Table S6. Correlation analysis between the background, laser cutting, lid opening, and post background of the OPS data for experimental method 3.

Method 3 - OPS		**Background**	**Laser Cutting**	**Lid Opening**	**Post Background**
Background	*Pearson*	1.00	0.999	0.999	0.999
	Sig.	2.2 E -16	2.2 E -16	2.2 E -16	2.2 E -16
	N	12	12	12	12
Laser Cutting	*Pearson*	0.999	1.00	0.999	0.999
	Sig.	2.2 E -16	2.2 E -16	8.2 E -16	2.2 E -16
	N	12	12	12	12
Lid Opening	*Pearson*	0.999	0.999	1.00	0.999
	Sig.	2.2 E -16	8.2 E -16	2.2 E -16	2.2 E -16
	N	12	12	12	12
Post Background	*Pearson*	0.999	0.999	0.999	1.00
	Sig.	2.2 E -16	2.2 E -16	2.2 E -16	2.2 E -16
	N	12	12	12	12

Table S7. Analysis of Variance (ANOVA) between total concentration means within the experimental methods. Note: Group mean refers to the average total concentration of each of the phases of the experimental method (i.e. background, laser cutting, lid opening, and post-background)

	Degrees of Freedom	P-value	F-crit
Method 1 SMPS	3	1.748E-11	2.79806064
Method 2 SMPS	3	4.4114E-17	2.79806064
Method 3 SMPS	3	3.9633E-16	2.79394885
Method 1 OPS	3	0.47287749	2.79806064
Method 2 OPS	3	2.4197E-08	2.79806064
Method 3 OPS	3	0.00295071	2.79394885

Table S8. Two sample t-test between background and post-background concentrations for each experimental method (assuming equal variance).

	Degrees of Freedom	P-value (one tail)	P-value (two-tailed)
Method 1 SMPS	38	0.09845998	2.02439416
Method 2 SMPS	38	2.25344E-14	4.50688E-14
Method 3 SMPS	38	1.8248E-13	3.6496E-13
Method 1 OPS	38	0.12476186	0.24952373
Method 2 OPS	38	2.8625E-06	5.7249E-06
Method 3 OPS	38	0.00047066	0.00094132

REFERENCES

(1) Keller, J. An Investigation of the Airborne Particulate Matter Related Health Hazards Present in Makerspaces. Bucknell University, Digital Commons, 2021.

(2) Badoniya, P. CO2 Laser Cutting of Different Materials-A Review. *International Journal of Engineering and Technical Research* **2018**, *5*, 2103-2115.

(3) Mushtaq, R. T.; Wang, Y.; Rehman, M.; Khan, A. M.; Mia, M. State-Of-The-Art and Trends in CO(2) Laser Cutting of Polymeric Materials-A Review. *Materials (Basel)* **2020**, *13* (17). DOI: 10.3390/ma13173839 From NLM.

(4) Radovanović, M.; Madić, M. Experimental investigations of CO2 laser cut quality: A review. *Nonconventional Technologies Review* **2011**, *15*.

(5) Haferkamp, H.; Alvensleben, F. v.; Seebaum, D.; Goede, M.; Püster, T. Air contaminants generated during laser processing of organic materials and protective measures. *Journal of Laser Applications* **1998**, *10* (3), 109-113. DOI: 10.2351/1.521835.

(6) Herrick, D.; Klein, R. Emerging Health and Safety Issues in Makerspaces ISAM 2016 Paper No. 2017.

(7) He, Y.; Xie, H.; Ge, Y.; Lin, Y.; Yao, Z.; Wang, B.; Jin, M.; Liu, J.; Chen, X.; Sun, Y. Laser Cutting Technologies and Corresponding Pollution Control Strategy. *Processes* **2022**, *10* (4), 732.

(8) *A world leader in fume and dust extraction systems*. Donaldson Filtration Solutions, 2022. (accessed 2022.

(9) Pawar, E. G. A Review Article on Acrylic PMMA. 2016.

(10) Zafar, M. S. Prosthodontic Applications of Polymethyl Methacrylate (PMMA): An Update. *Polymers (Basel)* **2020**, *12* (10). DOI: 10.3390/polym12102299 From NLM.

(11) Khoshaim, A. B.; Elsheikh, A. H.; Moustafa, E. B.; Basha, M.; Showaib, E. A. Experimental investigation on laser cutting of PMMA sheets: Effects of process factors on kerf characteristics. *Journal of Materials Research and Technology* **2021**, *11*, 235-246. DOI: https://doi.org/10.1016/j.jmrt.2021.01.012.

(12) Elsheikh, A. H.; Deng, W.; Showaib, E. A. Improving laser cutting quality of polymethylmethacrylate sheet: experimental investigation and optimization. *Journal of Materials Research and Technology* **2020**, *9* (2), 1325-1339. DOI: https://doi.org/10.1016/j.jmrt.2019.11.059.

(13) Kokosa, J. M. Hazardous chemicals produced by laser materials processing. *Journal of Laser Applications* **1994**, *6* (4), 195-201. DOI: 10.2351/1.4745357.

(14) Nho, R. Pathological effects of nano-sized particles on the respiratory system. *Nanomedicine* **2020**, *29*, 102242. DOI: 10.1016/j.nano.2020.102242 From NLM.

(15) Schraufnagel, D. E. The health effects of ultrafine particles. *Experimental & Molecular Medicine* **2020**, *52* (3), 311-317. DOI: 10.1038/s12276-020-0403-3.

(16) Kim, K. H.; Jahan, S. A.; Kabir, E.; Brown, R. J. A review of airborne polycyclic aromatic hydrocarbons (PAHs) and their human health effects. *Environ Int* **2013**, *60*, 71-80. DOI: 10.1016/j.envint.2013.07.019 From NLM.

(17) Armstrong, B.; Hutchinson, E.; Unwin, J.; Fletcher, T. Lung cancer risk after exposure to polycyclic aromatic hydrocarbons: a review and meta-analysis. *Environ Health Perspect* **2004**, *112* (9), 970-978. DOI: 10.1289/ehp.6895 From NLM.

(18) Yadav, I. C.; Devi, N. L. Biomass Burning, Regional Air Quality, and Climate Change. In *Encyclopedia of Environmental Health (Second Edition)*, Nriagu, J. Ed.; Elsevier, 2019; pp 386-391.

(19) Tsai, C.-J.; Huang, C.-Y.; Chen, S.-C.; Ho, C.-E.; Huang, C.-H.; Chen, C.-W.; Chang, C.-P.; Tsai, S.-J.; Ellenbecker, M. J. Exposure assessment of nano-sized and respirable particles at different workplaces. *Journal of Nanoparticle Research* **2011**, *13* (9), 4161-4172. DOI: 10.1007/s11051-011-0361-8.

(20) Sonwani, S.; Madaan, S.; Arora, J.; Suryanarayan, S.; Rangra, D.; Mongia, N.; Vats, T.; Saxena, P. Inhalation Exposure to Atmospheric Nanoparticles and Its Associated Impacts on Human Health: A Review. *Frontiers in Sustainable Cities* **2021**, *3*, Review. DOI: 10.3389/frsc.2021.690444.

(21) Nemmar, A.; Holme, J. A.; Rosas, I.; Schwarze, P. E.; Alfaro-Moreno, E. Recent advances in particulate matter and nanoparticle toxicology: a review of the in vivo and in vitro studies. *Biomed Res Int* **2013**, *2013*, 279371. DOI: 10.1155/2013/279371 From NLM.

(22) Kiefer, M.; Moss, C. E. Laser generated air contaminants released during laser cutting of fabrics and polymers. *Journal of Laser Applications* **1997**, *9* (1), 7-13. DOI: 10.2351/1.4745440.

(23) Tsai, C. S.-J.; Theisen, D. A sampler designed for nanoparticles and respirable particles with direct analysis feature. *Journal of Nanoparticle Research* **2018**, *20*, 209. DOI: 10.1007/s11051-018-4307-2.

(24) Spietelun, A.; Pilarczyk, M.; Kloskowski, A.; Namieśnik, J. ChemInform Abstract: Current Trends in Solid-Phase Microextraction (SPME) Fibre Coatings. *Chemical Society reviews* **2010**, *39*, 4524-4537. DOI: 10.1039/c003335a.

(25) Ouyang, G.; Pawliszyn, J. SPME in environmental analysis. *Analytical and bioanalytical chemistry* **2006**, *386*, 1059-1073. DOI: 10.1007/s00216-006-0460-z.

(26) Ott, E.-J. E.; Kucinski, T. M.; Dawson, J. N.; Freedman, M. A. Use of Transmission Electron Microscopy for Analysis of Aerosol Particles and Strategies for Imaging Fragile Particles. *Analytical Chemistry* **2021**, *93* (33), 11347-11356. DOI: 10.1021/acs.analchem.0c05225.

(27) Pósfai, M.; Axisa, D.; Tompa, É.; Freney, E.; Bruintjes, R.; Buseck, P. R. Interactions of mineral dust with pollution and clouds: An individual-particle TEM study of atmospheric aerosol from Saudi Arabia. *Atmospheric Research* **2013**, *122*, 347-361. DOI: https://doi.org/10.1016/j.atmosres.2012.12.001.

(28) Agency, E. P. Methyl Methacrylate. Agency, U. E. P., Ed.; Environmental Protection Agency: https://www.epa.gov/sites/default/files/2016-09/documents/methyl-methacrylate.pdf, 2000.